Appl Phys A (2010) 101: 533–538
DOI 10.1007/s00339-010-5892-9

Applied Physics A
Materials Science & Processing

Ablation of silicon suboxide thin layers

**M. Jahn · J. Richter · R. Weichenhain-Schriever ·
J. Meinertz · J. Ihlemann**

Received: 17 November 2009 / Accepted: 24 May 2010 / Published online: 3 July 2010

Abstract We investigate the ablation of SiO_x thin films on fused silica substrates using single-pulse exposures at 193 nm and 248 nm. Two ablation modes are considered: front side (the surface of a film is irradiated from above) and rear side (a film is irradiated through its supporting substrate). Fluence is varied from below 200 $\mathrm{mJ/cm^2}$ to above 3 $\mathrm{J/cm^2}$. SiO_x films of thickness 200 nm, 400 nm, and 600 nm are ablated. In the case of rear-side illumination, at moderate fluences (around 0.5 $\mathrm{mJ/cm^2}$) the ablation depth corresponds roughly to the film thickness, above 1 $\mathrm{J/cm^2}$ part of the substrate is ablated as well. In the case of front-side ablation the single-pulse ablation depth is limited for all film thicknesses to less than 200 nm even at fluences up to 4 $\mathrm{J/cm^2}$. Experimental results are discussed in relation to film thickness, fluence, and ablation mode. Simple numerical calculations are performed to clarify the influence of heat transport on the ablation process.

1 Introduction

Because of its high transparency throughout the UV/VIS/NIR spectral region fused silica ($\mathrm{SiO_2}$) finds widespread use in optical components. Excimer-grade fused silica has sufficiently high transmission to permit its use in laser optics even at 193 nm (ArF excimer laser). The small absorption in the DUV, however, makes processing of fused silica by excimer laser ablation rather difficult. While ablation at 193 nm is possible at high fluences (in excess of 2 $\mathrm{J/cm^2}$) the ablation rate is found to depend on the surface roughness and irradiation by multiple pulses can lead to crack formation [1]. Processing of fused silica at 157 nm ($\mathrm{F_2}$ laser) has been performed by a number of groups and interesting applications have been demonstrated [2–5]. The experimental effort, however, is very high: beam lines have to be evacuated or purged to remove any absorbing oxygen and laser optics have to be all-reflective or made from expensive materials like calcium fluoride. Also, the available pulse energy is normally less for $\mathrm{F_2}$ lasers.

To circumvent these problems indirect methods have been invented that permit processing of fused silica at standard excimer laser wavelengths. These methods employ an auxiliary medium which absorbs the UV laser photons and transfers some of the energy to the fused silica resulting in material removal. Some of these methods and variations thereof are known as *laser-induced backside wet-etching* (LIBWE) [6–8], *laser-induced plasma assisted ablation* (LIPAA) [9], *laser etching at a surface adsorbed layer* (LESAL) [10], and, more recently, *laser-induced backside dry etching* (LIBDE) [11]. LIBDE, which commonly uses metal absorbers, has been thoroughly studied [12, 13] and is a promising technique for laser microprocessing of transparent materials. In recent years we have developed an alternative method for excimer laser micromachining of fused silica [14]. As absorbing medium we use non-stoichiometric silicon oxide (SiO_x) thin films coated on fused silica substrates. SiO_x has sufficiently high absorption to permit ablation at 248 nm (KrF excimer laser) and 193 nm. After ablation the remaining SiO_x film can be oxidized to $\mathrm{SiO_2}$, e.g. by baking in an oven, yielding a UV-transparent component completely composed of $\mathrm{SiO_2}$ [15]. Baking takes around 8 hours for SiO_x films that are 200 nm thick. A 600 nm SiO_x film requires up to 24 hours of baking for complete oxidation so the method is better suited for thin films.

M. Jahn · J. Richter · R. Weichenhain-Schriever ·
J. Meinertz (✉) · J. Ihlemann
Laser-Laboratorium Göttingen e. V., Hans-Adolf-Krebs-Weg 1,
37077 Göttingen, Germany
e-mail: joerg.meinertz@llg-ev.de

In rear-side ablation (RSA) irradiation is performed through the substrate. The interface between the non-absorbing fused silica substrate and the absorbing SiO_x film then functions as a predetermined breaking point, so film ablation leaves behind the substrate surface which has a low roughness. The combination of rear-side SiO_x film ablation followed by oxidation to SiO_2 can be used to produce high-quality UV-transparent phase masks very cost-efficiently [16].

Though similar, our method differs from LIBDE in some key points. Firstly, laser processing is normally performed below the threshold for indirect ablation, i.e. the transparent substrate is not etched. And secondly, the remaining SiO_x film is left on the substrate and converted to SiO_2 by oxidation becoming an intrinsic part of the surface pattern. In LIBDE the film is removed by some wet-chemical agent. Therefore, etch depths for LIBDE directly refer to the transparent substrate. In our method, they refer to the film-on-substrate system. This is to be kept in mind when comparing both methods. In the following, results on front-side ablation (FSA) and RSA of SiO_x thin films are presented.

2 Experiment

Ablation experiments on silicon suboxide (SiO_x, $x < 2$) thin films were performed at 193 nm using a Lambda Physik LPX 300 ArF excimer laser and at 248 nm using a Lambda Physik EMG 300 MSC KrF excimer laser. Samples consisted of excimer-grade (UV-transparent) fused silica substrates coated with single layers of SiO_x of a prescribed thickness. For the samples discussed in this paper, the nominal film thickness ranges from 20 nm to 600 nm. Coating was performed by a commercial coating shop (Laseroptik, Garbsen, Germany). Although this coating shop labels the films as silicon monoxide ($x = 1$), the oxygen content x is not known exactly and may vary between samples belonging to different batches. However, all investigated films show strong absorption in the UV. Transmission measurements with a UV/VIS/NIR spectrometer (Perkin Elmer Lambda 19) on a 84 nm SiO_x film provided estimates of the absorption coefficient α of $4.6\times10^5\ \mathrm{cm}^{-1}$ at 193 nm and $2.7\times10^5\ \mathrm{cm}^{-1}$ at 248 nm. Film transmission in the VIS region is around 0.8 to 0.9 and shows Fabry-Pérot resonances originating from multiple reflections in the film. From these resonances and the known film thicknesses a crude (wavelength-independent) estimate of the refractive index of around 1.9 can be obtained. This is in good agreement with refractive index data for SiO graphed in [17] for the wavelength region from 240 nm to 1000 nm. Finally, film thickness increases by a factor of approximately 1.2 to 1.4 upon oxidation and UV-transmission rises to values characteristic of fused silica. This points to a significant incorporation of oxygen so it is reasonable to assume $1 \approx x \ll 2$ for the SiO_x films.

The ablation experiments were carried out using a mask-projection setup. Employed masks included simple geometries like circular apertures and slits as well as more complex ones like gratings and concentric rings. Depending on mask and demagnification ratio the obtained feature size of ablated structures ranged from a few to several hundred microns. Laser fluence was controlled with a variable attenuator, the energy of the laser pulses being measured using a standard joulemeter. FSA and RSA modes were investigated. In FSA mode the sample is mounted with the SiO_x film facing the incident laser beam while in RSA mode the laser pulse first travels through the fused silica substrate before being absorbed by the film. In this latter mode care has to be taken because the substrate leads to an axial shift of the projected mask image. This has been accounted for in the experiments. All ablations were carried out at room temperature and atmospheric pressure.

3 Results and discussion

Figure 1 shows confocal microscope images of cavities ablated in a 400 nm SiO_x film using FSA and RSA at 193 nm. For these results a chromium on calcium fluoride mask with a square aperture was imaged by a spherical lens onto the film at a demagnification of 10:1. The size of the aperture, $1 \times 1\ \mathrm{mm}^2$, was chosen so that inhomogeneities of the laser beam would have a negligible effect on the ablation results. Fluence was varied from around $200\ \mathrm{mJ/cm}^2$ to above $3\ \mathrm{J/cm}^2$. Around $350\ \mathrm{mJ/cm}^2$ FSA (Fig. 1a) and RSA (Fig. 1b) produce cavities with well-defined edges while around $3\ \mathrm{J/cm}^2$ FSA (Fig. 1c) and RSA (Fig. 1d) result in cavities with blurred edges. An obvious difference between Fig. 1c and Fig. 1d is the roughness of the cavity bottoms. The roughness resulting from FSA (Fig. 1c) is higher than that resulting from RSA (Fig. 1d). This observation holds over the whole investigated fluence range, irrespective whether just the film is ablated or part of the substrate, too—FSA produces rougher cavity bottoms than RSA. In fact, the confocal microscope data for FSA are so noisy that we have not been able to reliably quantify ablation depths while this would have been possible for most of the measurements on cavities produced by RSA. For this reason etch depths were determined independently with a Sloan Dektak 3030 stage profiler.

Figure 2 shows the obtained single-pulse etch depths for FSA and RSA of a 200 nm and a 400 nm SiO_x film at 193 nm. Also shown are data for FSA of a 200 nm and a 600 nm SiO_x film at 248 nm. From these data one can see that the ablation threshold for FSA is lower at 193 nm than at 248 nm. This is expected because of the stronger absorption of SiO_x at 193 nm. At 248 nm there is no ablation below

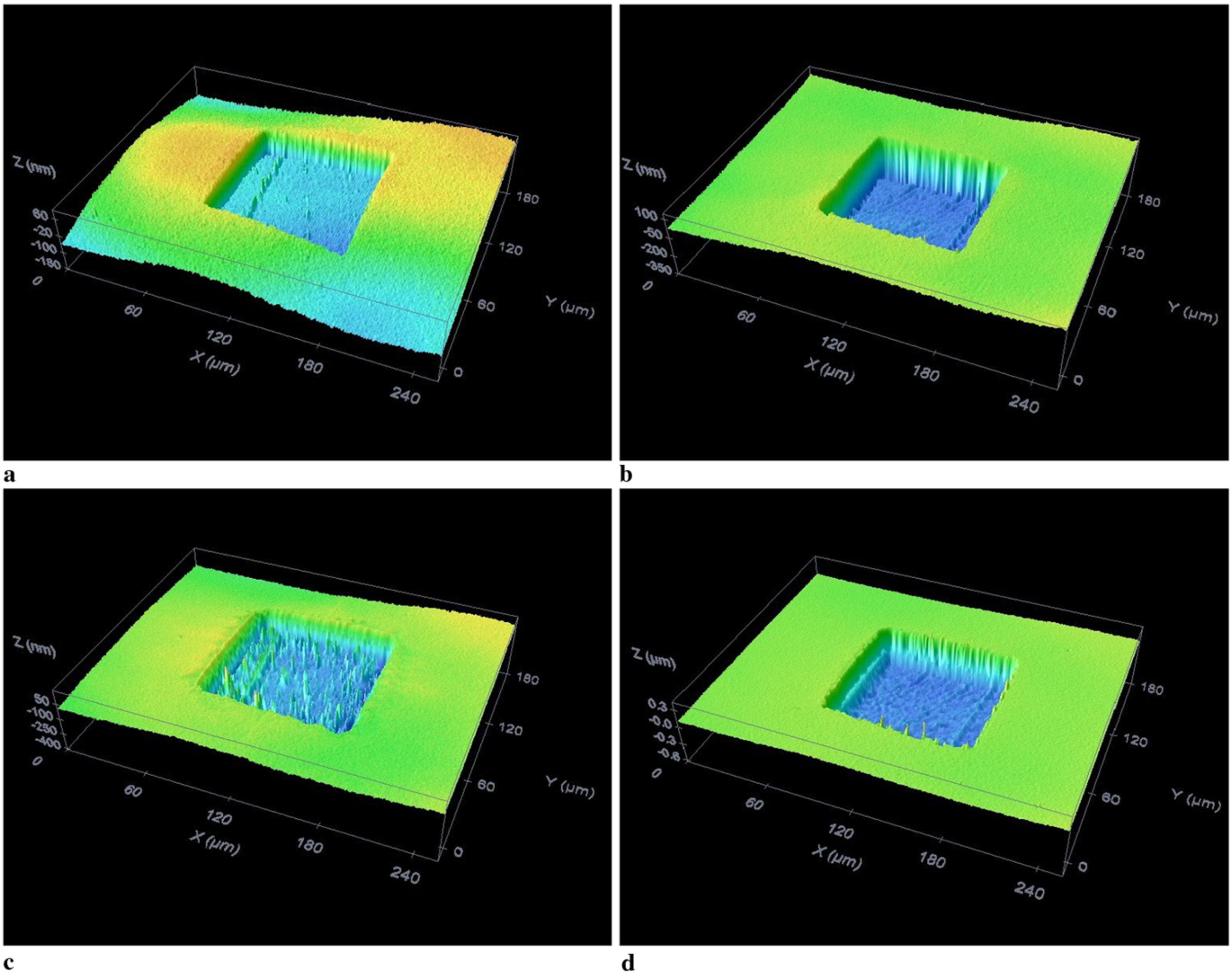

Fig. 1 Single-pulse ablation of a 400 nm thick SiO_x film at 193 nm; (**a**) FSA, 370 mJ/cm^2; (**b**) RSA, 340 mJ/cm^2; (**c**) FSA, 3.2 J/cm^2; (**d**) RSA, 3.0 J/cm^2. Measurements by confocal microscope. Note different z scales

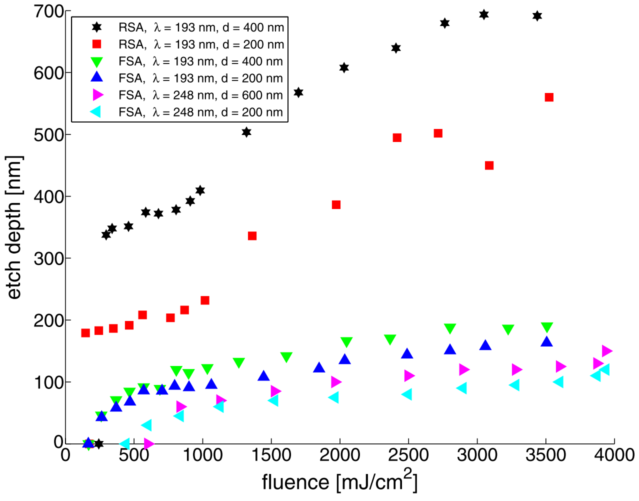

Fig. 2 Single-pulse ablation depth versus fluence for SiO_x films of varying thickness; λ: wavelength; d: film thickness

500 mJ/cm^2. At 193 nm single-pulse etch depths of 43 nm (200 nm film) and 47 nm (400 nm film) are observed around 260 mJ/cm^2 while no ablation is observed at 170 mJ/cm^2 (both films). Between 170 mJ/cm^2 and 260 mJ/cm^2 data obtained from the stage profiler are inconclusive because the irradiated area becomes rougher before ablation sets in. This is supported by the confocal microscope measurements. The etch depth increases with fluence for both wavelengths and all films. However, for FSA, measured etch depths remain below the film thickness in all cases, at least within the fluence range of this study. We believe the main reason for this is plasma shielding of the laser pulse by the ablation plume. The largest etch depths measured for FSA at 193 nm were 190 nm (3.5 J/cm^2, 400 nm film) and 163 nm (3.5 J/cm^2, 200 nm film). For FSA at 248 nm the data are 150 nm (3.9 J/cm^2, 600 nm film) and 120 nm (3.9 J/cm^2, 200 nm film). One final observation about the data on FSA is that, firstly, for a fixed fluence ablation depths are consistently

larger at 193 nm than at 248 nm and, secondly, that for a fixed fluence and wavelength ablation depths are consistently larger for thicker than for thinner films. The first effect is more pronounced than the second. The reasons for this are still under investigation. With respect to the thickness dependence it has to be noted, however, that because of roughness the measurement error of the ablation depth is of the same order of magnitude as the differences observed in the data. Therefore, this effect is hard to verify experimentally.

For RSA at 193 nm incomplete film removal is observed at 174 $\mathrm{mJ/cm^2}$ for the 200 nm SiO_x film and at 297 $\mathrm{mJ/cm^2}$ for the 400 nm film. In some parts of the irradiated area the film is removed, in others it is still on the substrate. Complete film removal is observed at 243 $\mathrm{mJ/cm^2}$ (200 nm film) and at 340 $\mathrm{mJ/cm^2}$ (400 nm film). For completeness we also mention data obtained in our lab for RSA at 248 nm. Complete removal of an SiO_x film 200 nm thick requires around 400 $\mathrm{mJ/cm^2}$ while around 600 $\mathrm{mJ/cm^2}$ are needed for a 600 nm film. A 20 nm SiO_x film can be ablated with around 200 $\mathrm{mJ/cm^2}$. These data strongly suggest that there is a positive correlation between film thickness and threshold fluence required for complete film removal, i.e. thicker films require more fluence in RSA. In the low fluence region where complete film removal begins, measured ablation depths come out about 10 percent lower than the nominal film thickness. This suggests that some SiO_x remains on the substrate or is redeposited there during the ablation. With increasing fluence ablation depths first rise slowly, then, at some fluence the ablation depth exceeds the film thickness. From there, ablation depths rise faster with fluence. In this latter regime the substrate is etched. As can be seen for the 200 nm film this etching of the fused silica substrate can be very effective. At 3.5 $\mathrm{J/cm^2}$ the measured single-pulse ablation depth is 560 nm which means that 360 nm $\mathrm{SiO_2}$ have been removed in addition to 200 nm SiO_x. It is worthy to note that one does not depend on an SiO_x layer that thick for this effect. A study conducted in our group has demonstrated ablation rates of several hundred nanometers with single-pulse RSA and an absorbing SiO_x film only 28 nm thick [18].

Figure 3 shows a binary structure of alternating lines and spaces produced by RSA of a 223 nm thick SiO_x layer. For this structure a chromium on quartz mask was demagnified four times by a 4×/10-248 objective (MicroLas, Göttingen, Germany). Ablation was performed at 248 nm using just a single laser pulse. The average fluence, obtained by dividing the measured pulse energy by the total area of the structure, was 200 $\mathrm{mJ/cm^2}$. At a fill factor of 0.5 this gives a calculated fluence of 400 $\mathrm{mJ/cm^2}$ on the grating lines. The single pulse produced a grating with a period of only 2 µm covering an area of 4.7 $\mathrm{mm^2}$. Figure 3 shows some of the grating lines. Their edges are well-defined so that the structure is indeed binary, i.e. step-function like with two levels defined by the SiO_x–air and SiO_x–substrate interfaces. This result demonstrates that binary microstructures covering areas of multiple square millimeters and with feature sizes on the micron level can be efficiently produced by single-pulse RSA of SiO_x layers.

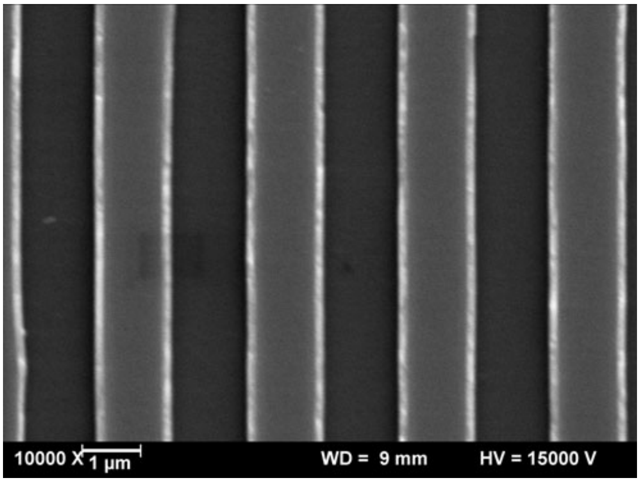

Fig. 3 Binary structure of alternating 1 µm wide ridges and trenches produced by single-pulse RSA at 248 nm of a 223 nm thick SiO_x layer. 200 $\mathrm{mJ/cm^2}$ average fluence (pulse energy divided by area of grating) corresponding to 400 $\mathrm{mJ/cm^2}$ on the grating lines

We have used a simple thermal model to qualitatively analyze our results. To that end, we have numerically solved the heat-transport equation

$$\rho c_p \frac{\partial T}{\partial t} = \kappa \frac{\partial^2 T}{\partial z^2} + \alpha I(z,t) \tag{1}$$

for a film-on-substrate system irradiated by a laser pulse. Because the irradiated area is large compared to the film thickness, lateral heat conduction is neglected and only the longitudinal coordinate z is kept. $T(z,t)$ and $I(z,t)$ are the temperature and laser intensity, respectively. We treat the density ρ, the specific heat capacity c_p, the thermal conductivity κ and the absorption coefficient α as constants (which were allowed to differ between film and substrate). The film surface is taken as an isolating interface which does not permit heat flow and the substrate is modeled as a 2000 nm thick layer in contact with a heat bath at room temperature. Used parameter values are $\rho = 2.13\ \mathrm{g/cm^3}$ [19] for SiO_x, $\rho = 2.20\ \mathrm{g/cm^3}$ [20] for fused silica, $c_p = 1.052\ \mathrm{J/(g\,K)}$ [20] for fused silica $\kappa = 0.015\ \mathrm{W/(cm\,K)}$ [20] for fused silica $\alpha = 2.7 \times 10^5\ \mathrm{cm^{-1}}$ for SiO_x at 248 nm (own estimate from transmission spectra), and $\alpha = 0$ for $\mathrm{SiO_2}$ (idealization of a non-absorbing substrate). Lacking data on SiO_x for c_p and κ the parameter values for fused silica are used which represents a further simplification within the used model. The laser pulse is modeled as a $\tau = 20$ ns Gaussian pulse.

First, we consider ablation at 248 nm of a 20 nm thick SiO_x film. In this case, the film thickness is less than the absorption length α^{-1} of around 40 nm and significantly less than the thermal diffusion length $\sqrt{\kappa\tau/(\rho c_p)}$ of around 100 nm. Not surprisingly, heat equilibration is so rapid that the temporal dependence of the temperature is nearly identical at all depths z within the film which means that the same maximum temperature is reached throughout the film. This result is in agreement with the experimental observation that no discernible difference is observed in the threshold fluence for FSA and RSA. Thus, the model supports the hypothesis that ablation of SiO_x films in this thickness range comprises melting and evaporation of the whole film regardless of ablation mode. For thicker films and FSA, the numerical results do not suggest an influence of film thickness on the ablation process. Temperatures calculated for a 200 nm and a 400 nm film are similar. Thus, our simple thermal model would suggest that FSA of these films is not different from bulk ablation which is in fair agreement with the experimental results shown in Fig. 2. This behavior is different from that observed for metal films of a similar thickness where the threshold fluence for ablation is thickness-dependent [21]. Because of the higher thermal conductivity heat equilibrates more rapidly in a metal film and is effectively confined there if the supporting substrate has a lower thermal conductivity as is the case for fused silica. In SiO_x heat equilibration is slower and, thus, large thermal gradients can build up during irradiation by the laser pulse. The maximum temperature reached during irradiation is highest at the film surface and drops with increasing depth into the film, falling below the threshold required for ablation at some distance from the surface.

For RSA the situation is a bit different. In this ablation geometry, the laser pulse heats a small zone near the film-substrate interface. From this zone heat can flow away into the substrate and into the film The heat flux in the film terminates, however, at the front film surface which serves as an isolating barrier. For thin films this can lead to an accumulation of heat so that a higher temperature is reached at the film-substrate interface than would be the case in thicker films. We investigate this effect with respect to a simple model view of the ablation process. From our experimental results we hypothesize that RSA of thick SiO_x films does not involve melting and evaporation of the whole film but is better characterized as a process where only a thin layer near the substrate evaporates resulting in delamination of the film. Then, we calculate the laser fluence required to reach a threshold temperature at the film–substrate interface in dependence of the film thickness. Lacking data for SiO_x, we arbitrarily take this threshold temperature as the evaporation temperature of SiO, given as 1880°C in [22] (the melting temperature according to that reference is $>1700°C$). The calculated threshold fluence using this simple model does show a dependence on film thickness, being smaller for thinner films and reaching a constant value for thick films. However, compared to the experimental values the calculated threshold fluences come out a factor of 2 to 3 too low and stagnate at too low film thicknesses. This indicates that a detailed analysis has to take additional effects into account that are non-thermal. Mechanical effects might be important in this respect.

4 Conclusion

Our results demonstrate that single-pulse RSA of SiO_x thin films on fused silica is a practical method to produce SiO_x-on-SiO_2 or (by oxidation) all-SiO_2 microstructures by excimer laser micromachining at 193 nm and 248 nm. For a given wavelength and film thickness a fluence range exists where RSA results in removal of the SiO_x film without damage to the supporting substrate. Within that range, obtained etch depths are equal to within about 10 percent, the remaining slight fluence dependence being an interesting open question. Above that range, significant etching of the substrate occurs at 193 nm, which might itself be a useful effect for micromachining of fused silica. For a given wavelength the threshold fluence required for RSA of SiO_x thin films shows a clear dependence on film thickness. Analysis using a simple thermal model hints at heat diffusion playing a part in this effect, but a more detailed description is necessary, which possibly needs to take into account mechanical effects within the film-substrate system.

Acknowledgement Financial support by the German Federal Ministry of Economics and Technology (grant no. 16IN0505) is gratefully acknowledged.

References

1. J. Ihlemann, M. Schulz-Ruhtenberg, T. Fricke-Begemann, J. Phys. Conf. Ser. **59**, 206 (2007)
2. P.R. Herman, R.S. Marjoribanks, A. Oettl, K. Chen, I. Konovalov, S. Ness, Appl. Surf. Sci. **154–155**, 577–586 (2000)
3. J. Ihlemann, S. Müller, S. Puschmann, D. Schäfer, M. Wei, J. Li, P.R. Herman, Appl. Phys. A **76**, 751 (2003)
4. A.A. Tseng, Phys. Stat. Solidi A **204**, 709 (2007)
5. J. Dou, J. Li, P.R. Herman, J.S. Aitchison, T. Fricke-Begemann, J. Ihlemann, G. Marowsky, Appl. Phys. A **91**, 591 (2008)
6. J. Wang, J. Niino, A. Yabe, Appl. Phys. A **68**, 111–113 (1999)
7. K. Zimmer, R. Böhme, B. Rauschenbach, J. Laser Micro/Nanoeng. **1**, 292 (2006)
8. Y. Kawaguchi, H. Niino, T. Sato, A. Narazaki, R. Kurosaki, J. Phys. Conf. Ser. **59**, 380 (2007)
9. J. Zhang, K. Sugioka, K. Midorikawa, Opt. Lett. **23**, 1486–1488 (1998)
10. K. Zimmer, R. Böhme, B. Rauschenbach, Appl. Phys. A **79**, 1883-1885 (2004)
11. B. Hopp, Cs. Vass, T. Smausz, Appl. Surf. Sci. **253**, 7922 (2007)
12. T. Smausz, T. Csizmadia, N. Kresz, Cs. Vass, Zs. Márton, B. Hopp, Appl. Surf. Sci. **254**, 1091 (2007)
13. B. Hopp, T. Smausz, T. Csizmadia, J. Budai, A. Oszkó, G. Szabó, J. Phys. D **41**, 175501 (2008)

14. M. Schulz-Ruhtenberg, J. Ihlemann, J. Heber, Appl. Surf. Sci. **248**, 190 (2005)
15. J.-H. Klein-Wiele, J. Békési, P. Simon, J. Ihlemann, JLMN—J. Laser Micro/Nanoeng. **1**, 211 (2006)
16. J. Ihlemann, R. Weichenhain-Schriever, J. Laser Micro/Nanoeng. **4**, 100 (2009)
17. G. Hass, C.D. Salzberg, J. Opt. Soc. Am. **44**, 181–187 (1954)
18. J. Ihlemann, Appl. Phys. A **93**, 75 (2008)
19. German Wikipedia on silicon monoxide: http://de.wikipedia.org/wiki/Siliciummonoxid
20. Heraeus Quarzschmelze, Transparent and Opaque Fused Silica, Document Q-A 1/112.2
21. E. Matthias, M. Reichling, J. Siegel, O.W. Käding, S. Petzold, H. Skurk, P. Bizenberger, E. Neske, Appl. Phys. A **58**, 129–136 (1994)
22. R.C. Weast, M.J. Astle, *CRC Handbook of Chemistry and Physics*, 64th edn. (CRC Press, Boca Raton, 1983)